Computational Diagnostic Techniques for Electromagnetic Scattering: Analytical Imaging, Near Fields, and Surface Currents

Kam W. Hom, Noel A. Talcott, Jr.
NASA Langley Research Center
Hampton, Virginia 23665

John Shaeffer
Marietta Scientific, Inc.
376 Powder Springs St., Suite 240A
Marietta, Georgia 30064
(770) 425-9760

ABSTRACT

This paper presents three techniques and the graphics implementations which can be used as diagnostic aides in the design and understanding of scattering structures: Imaging, near fields, and surface current displays. The imaging analysis is a new bistatic **k** space approach which has potential for much greater information than standard experimental approaches. The near field and current analysis are implementations of standard theory while the diagnostic graphics displays are implementations exploiting recent computer engineering work station graphics libraries.

INTRODUCTION

The goals and motivation of this work are to provide insight and guidance into the design of scattering structures. Analytical/computer codes have historically been conceived only to provide predictions of experimentally measured quantities, i.e., backscatter RCS versus angle. In principle, an analytical code should be able to provide a much greater insight into the scattering process if we just ask the proper questions. Our inspiration is similar to efforts in computational fluid dynamics where we are attempting to better understand the interaction of an EM wave with a structure, the nature of the scattering process, and ultimately better design.

BISTATIC IMAGE ANALYSIS USING k SPACE CONCEPTS

The experimental development of microwave images has been a powerful tool to understand scattering from various geometries. Imaging may be in one dimension, i.e., down range; or in two dimensions, i.e., down and cross range. This capability allows one to understand the scattering process in

terms of specific scattering centers and mechanisms. Image development has been mostly experimental. While one could apply the same methods to predictive scattering algorithms, the computation burden has always been considered to great. This occurs because, experimentally, down range information is obtained by illuminating the target over a bandwidth of frequencies typically numbering 16, 32, 64, 128 or even 512. To do this with a method of moments analysis, one would have to recompute and solve the system matrix for each frequency. This computation burden is so great that the swept frequency approach is seldom pursued analytically.

B. A. Cooper developed a new approach that requires only one computation of induced currents and therefore only one MOM matrix computation for down range images. A formal bistatic k space image theory was then developed, reference 1. This formulation is not limited by the small angle focus requirement. Cross range images are computed without smearing. The bistatic k space analytical image technique does not require a MOM code matrix solution for each frequency. Only one current distribution (matrix computation) is computed at the frequency of interest. The image is the Fourier transform of the k space bistatic scattered radiation for values of $\mathbf{k}^{scat}$ that correspond to downrange and cross range. The natural Fourier transform variables are wave number $\mathbf{k}$ and spatial position $\mathbf{R}$. If we compute a bistatic field as a function of $\mathbf{k}^{scat} = (k^{downrange}, k^{cross\ range})$ then the Fourier transform of the scattered field is naturally a function of the transformed spatial coordinates, $\mathbf{R}^{scat} = (R^{downrange}, R^{cross\ range})$. The computation of the scattered field in k space is a generalization of the standard bistatic radiation integral. The difference is that E^{scat} is computed in term of $\mathbf{k}^{scat}$ for down and/or down/cross range rather than in terms of the usual bistatic angles (θ,ϕ). Body currents are computed only once at the user specified incident angle and polarization.

Bistatic k space image technique features are: 1) Resolution up to $\lambda/2$ unlimited by the usual experimental frequency and angle extent bandwidth concerns; 2) Image focus / smear does not occur due to the formulation of the approach; 3) Images computed at the frequency and angle of body excitation. The body currents are computed only for this $\mathbf{k}^{inc}$. In contrast to the experimental approach, the currents do not change with changes in the bistatic $\mathbf{k}^{scat}$ vector sweep; 4) One, two, or three dimensional images may be obtained. The limiting feature for obtaining 3D images is the display of the solution since multidimensional FFT algorithms are available; 5) The scattering body is imaged in a bistatic sense from the same direction as the excitation, i.e., a backscatter image. However, a more general bistatic approach is entirely possible since the center of $\mathbf{k}^{scat}$ is not required to be the negative of $\mathbf{k}^{inc}$; and 6) A co or cross polarized image may be computed.

This list shows that *the bistatic analytical approach to imaging can potentially yield substantially more information than experimental images. The bistatic image approach can be applied to any predictive algorithm for electromagnetic scattering or antenna radiation, e.g., Physical Optics or Method of Moments.*

Briefly, the theory for this analytical imaging technique can be developed as follows. A current distribution is computed for a given angle of excitation and polarization. A scattered field is computed using the far field radiation integral as a function of down and cross range bistatic k directions,

$$E^{\alpha,\beta}(\vec{k}^{inc},\vec{k}^{scat}) = \int \{\hat{n}^{\alpha} \bullet \vec{J}^{\beta}(\vec{k}^{inc})\}\, e^{j\vec{k}^{scat}\bullet\vec{R}}\, dS \qquad \mathbf{1}$$

where α and β are the polarization of the scattered and incident field, $\mathbf{k}^{inc}$ is the direction of the incident excitation, and $\mathbf{k}^{scat}$ is the k space direction for the scattered field. This equation is the usual radiation integral as written before specifying $\mathbf{k}^{scat}$ as a function of look angle (θ,ϕ). We compute E as a function of $\mathbf{k}^{scat} = \mathbf{k}^{downrange} + \mathbf{k}^{crossrange}$. The downrange k is centered on the free space absolute value of $\mathbf{k}^{inc}$

$$k_r = \frac{2\pi}{\lambda_0} \pm \Delta k \qquad \mathbf{2}$$

The Fourier transform of this E field, computed in down and cross range k space, is our desired image,

$$E^{\alpha,\beta}\left(r_{down}, r_{cross}\right) = \int \left\{ \int W(\vec{k}^{\,s})\, E^{\alpha,\beta}(\vec{k}^{\,inc}, \vec{k}^{\,scat})\, e^{j\vec{k}_{down}\bullet\vec{R}}\, \mathrm{dk}_{\mathrm{down}}^{scat} \right\} e^{j\vec{k}_{cross}\bullet\vec{R}}\, \mathrm{dk}_{\mathrm{cross}}^{scat}$$

3

where W is a weight function and the square magnitude of E is our down/cross range image. It is noted that the computational cost of this process is *cheap* compared to the effort in a MOM code to compute **J**.

NEAR FIELDS and CURRENTS

The computation of near fields must resort back to the fundamental definition for fields rather than the simpler far field expression. The currents **J** are, of course, computed by a MOM code as part of the solution. The near fields are specified in terms of the vector and scalar potentials in terms of the current distribution:

$$\vec{E}^{\,scat}(\vec{r}_f) = -jk\eta \int \left\{ \vec{J} - (\nabla_s \cdot \vec{J})(1 + jkR)(\vec{r}_f - \vec{r}_s)/(kR)^2 \right\} g\, dS$$

4

where the integral is over the source currents and g is the Greens' function.

The currents **J** and fields **E** are time varying vector quantities. We may choose to display the two time quadrature values, the real and imaginary parts, which correspond to 0 and -90 degrees phase, or to display the time animation of these vectors as

$$\vec{E}(\vec{r}, \omega t) = \Re\left\{\vec{E}(\vec{r})\right\}\cos(\omega t) - \Im\left\{\vec{E}(\vec{r})\right\}\sin(\omega t) \qquad \mathbf{5}$$

by letting ωt vary from 0 to 2π, or to compute a time average root mean square

$$E_{rms} = \frac{(\vec{E} \cdot \vec{E}^{*})^{1/2}}{\sqrt{2}} \qquad \mathbf{6}$$

For the E field quantities, we can display the scattered field, or the total field (sum of incident plus scattered), or just the incident field (not very interesting).

DIAGNOSTIC GRAPHICS DISPLAYS

Continued development of very fast engineering workstations has enabled the everyday use of graphics to visually display the EM vector and scalar quantities for fields, currents, and images. Visual display of the data includes color coded contour maps of the surface current magnitudes and the total and scattered electric field magnitudes for both RMS averages and time harmonic animation. The current and electric field vectors can be overlaid on this mapping or displayed separately to show field orientation and direction. The graphics program presently is capable of displaying and animating up to 50 planar cuts of a 100 x 100 field point matrix either simultaneously or individually. In addition, the program can display the triangle element mesh (up to 10,000 elements) which contains the surface current information. FORTRAN graphics routines have been developed for Silicon Graphics series workstations.

EXAMPLE

The techniques described herein have been incorporated into the MOM code of reference 2 which was used for the 3λ aircraft like geometry shown in Figure 1. The traditional backscatter computation is shown in Figure 2 for horizontal and vertical polarization.

Bistatic k-space images for the scattering centers when viewed nose on is shown in Figure 3 for both polarization's. Scattering centers at this angle are the engine pods, wing roots, and leading and trailing edges.

Surface currents for nose on horizontal polarization illumination is shown in Figure 4. The high current regions are the sides of the fuselage, the leading edges of the wing and horizontal fin, and the wing root region.

Near total electric fields about the target is shown in Figure 5 for nose on horizontal polarization illumination.

WHAT WE CAN LEARN

Imaging yields great insight into the scattering mechanism process, i.e., specular scattering, end region contribution, leading and trailing edge diffraction, traveling wave, creeping wave, edge wave scattering, etc. This new technique allows us to utilize imaging with computational MOM codes with little additional computational cost. In addition, we have the potential to do three dimensional images, bistatic imaging, and cross polarized imaging (even for circular polarization). Resolutions approaching $\lambda/2$ are possible. In fact, early efforts used resolutions less than $\lambda/2$ so that images of the MOM code basis functions were observed. Because the analytical approach is different from the swept frequency experimental approach, we have seen some differences in images, particularly for traveling wave scattering mechanisms where this new approach shows radiation as emanating from an extended region over which a reflected surface wave is propagating.

Current display diagnostics allow us to highlight regions of high and low current flow over a body. Low current regions could then be noted for possible addition of secondary structures such as vents, doors, or avionics sensors such that they would have minimum impact on scattering. In addition, one could gauge the design success of resistive treatments along edges and at tips by examining residual current levels and the taper function.

Near field plots have potential to examine the over all influence of the body structure on the field incident on secondary structures such as inlets and exhaust cavities. Since the main body influences the field, the polarization incident on secondary structure may not be that of the incident free space illumination.

As with any set of new tools, we do not fully know the potential benefit of all that is now possible. Clearly, images are of great value. Current and field knowledge help in our understanding of the scattering mechanisms, but we may have to be creative in how we use these diagnostics to exploit their full potential.

REFERENCES

1. J. F. Shaeffer, Kam W. Hom, R. Craig Baucke, Brett A. Cooper, and Noel A. Talcott, Jr., “Bistatic k-Space Imaging for Electromagnetic Prediction Codes for Scattering and Antennas,” NASA Technical Paper 3569, July 1996.

2. J. F. Shaeffer, “MOM3D Method of Moments Code Theory Manual,” NASA CR-189594, NAS1-18603, March 1992.

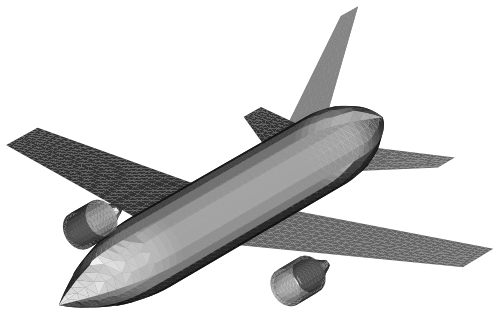

Figure 1 - Three wavelength aircraft geometry.

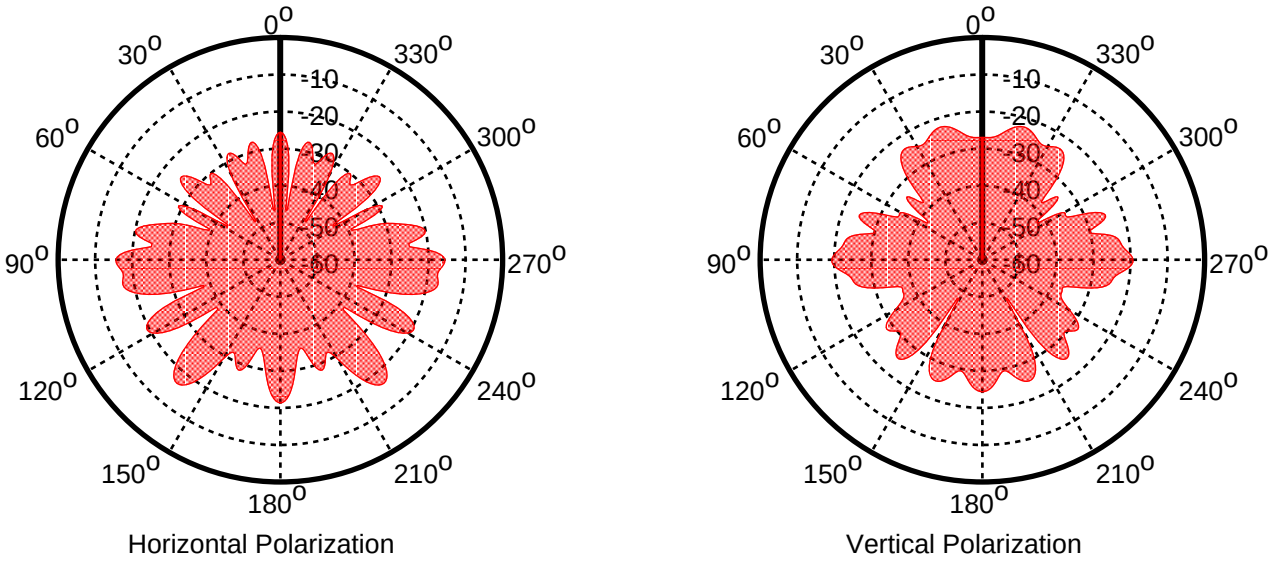

Figure 2 - Backscatter RCS plots of three wavelength aircraft geometry, horizontal and vertical polariztion, 0^{o} elevation.

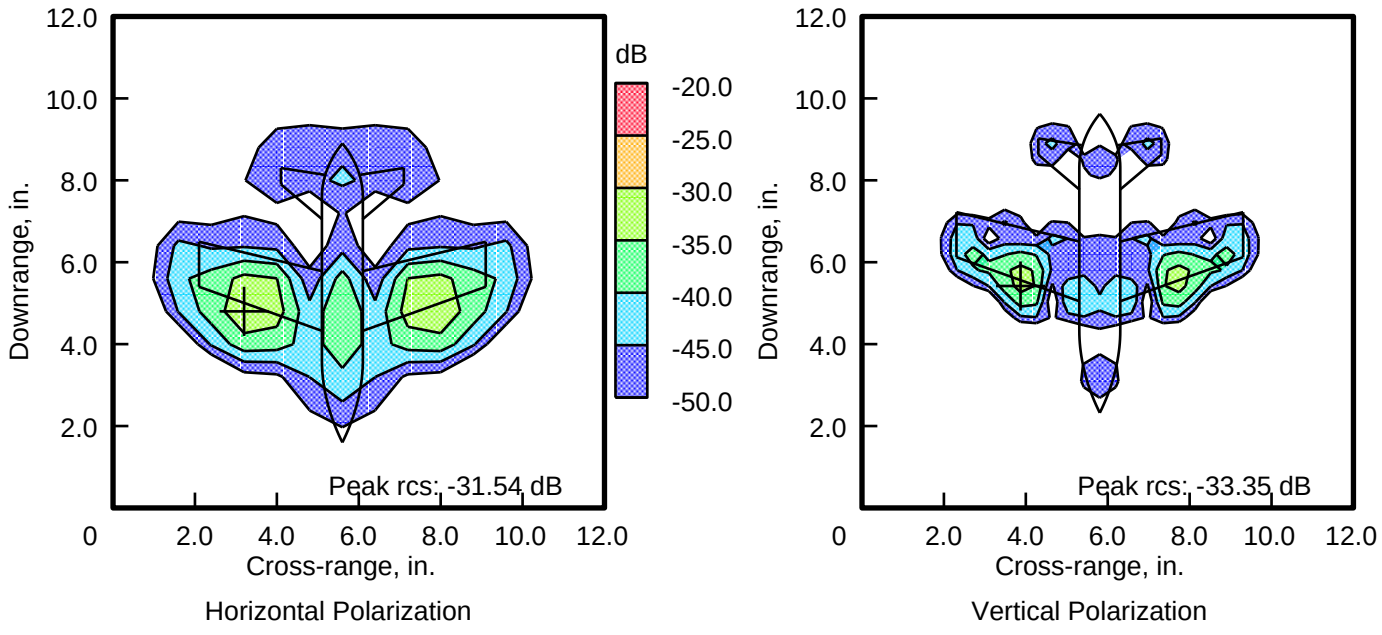

Figure 3 - Bistatic images of three wavelength aircraft geometry, horizontal and vertical polarization, 0^{o} elevation, 0^{o} azimuth.

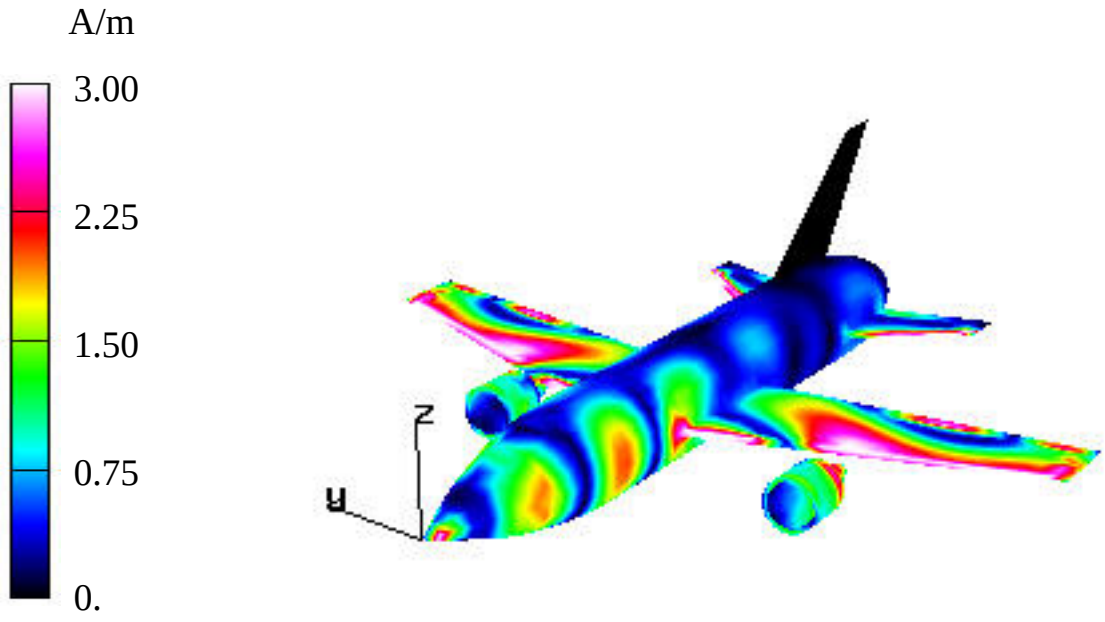

Figure 4 − Surface currents on three wavelength aircraft geometry, horizontal polarization, 0º elevation, 0º azimuth.

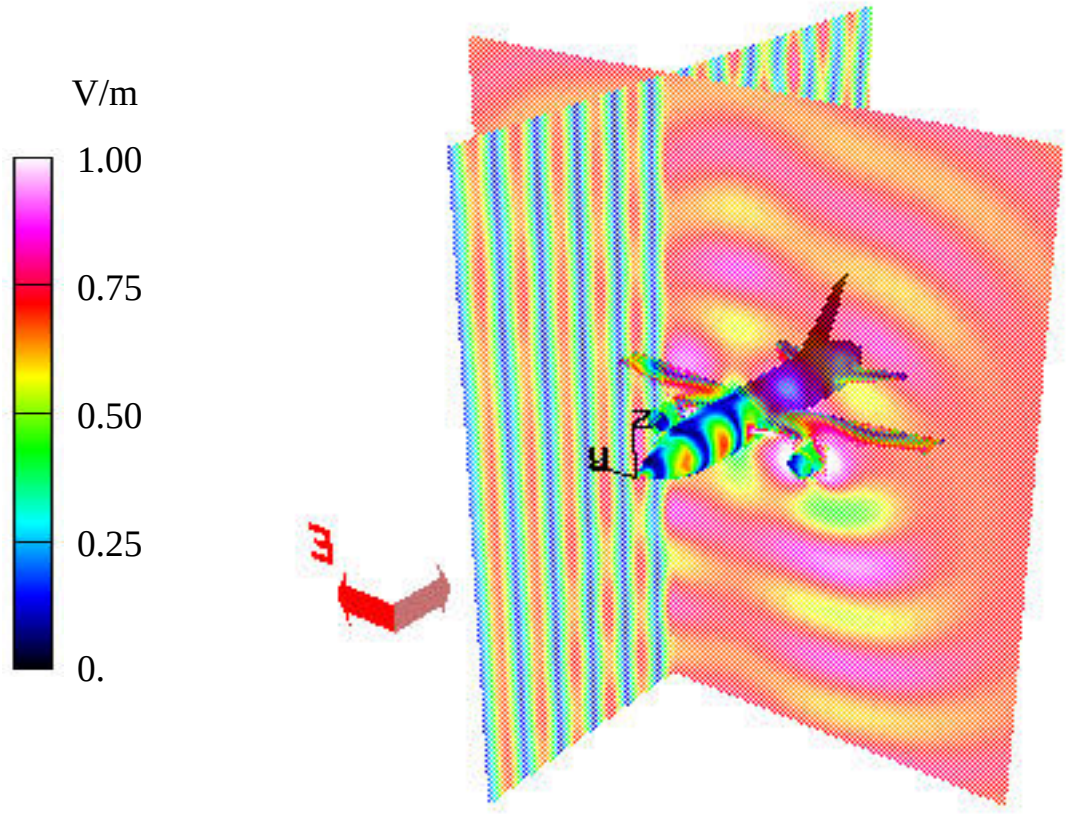

Figure 5 − Total electric field about three wavelength aircraft geometry, horizontal polarization, 0º elevation, 0º azimuth.